An Estimation of Turbulent Characteristics in the Low-Level Region of Intense Hurricanes Allen (1980) and Hugo (1989)

JUN A. ZHANG

Rosenstiel School of Marine and Atmospheric Science, University of Miami, and NOAA/AOML Hurricane Research Division, Miami, Florida

FRANK D. MARKS

NOAA/AOML Hurricane Research Division, Miami, Florida

MICHAEL T. MONTGOMERY

Naval Postgraduate School, Monterey, California, and NOAA/AOML Hurricane Research Division, Miami, Florida

SYLVIE LORSOLO

Rosenstiel School of Marine and Atmospheric Science, University of Miami, and NOAA/AOML Hurricane Research Division, Miami, Florida

(Manuscript received 29 March 2010, in final form 29 October 2010)

ABSTRACT

This study analyzes the flight-level data collected by research aircraft that penetrated the eyewalls of category 5 Hurricane Hugo (1989) and category 4 Hurricane Allen (1980) between 1 km and the sea surface. Estimates of turbulent momentum flux, turbulent kinetic energy (TKE), and vertical eddy diffusivity are obtained before and during the eyewall penetrations. Spatial scales of turbulent eddies are determined through a spectral analysis. The turbulence parameters estimated for the eyewall penetration leg are found to be nearly an order of magnitude larger than those for the leg outside the eyewall at similar altitudes. In the low-level intense eyewall region, the horizontal length scale of the dominant turbulent eddies is found to be between 500 and 3000 m, and the corresponding vertical length scale is approximately 100 m. The results suggest also that it is unwise to include eyewall vorticity maxima (EVM) in the turbulence parameter estimation because the EVMs are likely to be quasi-two-dimensional vortex structures that are embedded within the three-dimensional turbulence on the inside edge of the eyewall.

This study is a first attempt at estimating the characteristics of turbulent flow in the low-level troposphere of an intense eyewall using in situ aircraft observations. The authors believe that the results can offer useful guidance in numerical weather prediction efforts aimed at improving the forecast of hurricane intensity. Because of the small sample size analyzed in this study, further analyses of the turbulent characteristics in the high-wind region of hurricanes are imperative.

1. Introduction

Turbulent transport processes are believed to play an important role in the intensification and maintenance of a hurricane vortex (e.g., Emanuel 1995, 1997; Persing and Montgomery 2003; Smith et al. 2008; Bryan and Rotunno 2009a; Rotunno et al. 2009). However, because of safety constraints, direct measurements of turbulence in the inner-core region of intense hurricanes have been essentially nonexistent and observational efforts have been focused almost exclusively outside the eyewall region. Turbulence measurements in the high-wind region of the storm would enable a proper assessment of subgrid-scale parameterizations, which include boundary layer parameterizations, used in numerical models for hurricane intensity prediction (e.g., Braun and Tao 2000; Nolan et al. 2009a,b; Smith and Thomsen 2010).

Moss and Merceret (1976, 1977) and Moss (1978) described one stepped-descent flight pattern in the boundary layer of the periphery of Tropical Storm Eloise. This

Corresponding author address: Jun Zhang, University of Miami/CIMAS, 4301 Rickenbacker Causeway, Miami, FL 33149.
E-mail: jun.zhang@noaa.gov

DOI: 10.1175/2010MWR3435.1

research flight measured momentum fluxes at different levels. Almost 30 yr later, the Coupled Boundary Layer Air–Sea Transfer (CBLAST) Experiment conducted during the 2002–04 hurricane seasons provided valuable data that contain measurements of turbulent fluxes of both momentum and enthalpy in the hurricane boundary layer between the outer rainbands (e.g., Black et al. 2007; Drennan et al. 2007; French et al. 2007; Zhang et al. 2008). However, all of these boundary layer turbulence observations have been restricted to surface wind speeds <30 m s^{-1} and to regions well outside the eyewall.

Using the data collected by a National Oceanic and Atmospheric Administration (NOAA) WP-3D research aircraft (N42RF hereafter) during the eyewall penetration of category 5 Hurricane Hugo (1989) at an altitude of around 450 m, Marks et al. (2008) recently presented the first in situ observations of the structure and evolution of the coherent vortex features in the eyewall, such as the eyewall vorticity maximum (EVM), which was observed to be on the inner edge of the eyewall reflectivity maximum. During the eyewall penetration, N42RF was flying within the inflow layer according to the Doppler radar observations.

The flight-level data collected during this Hugo mission are among the very few measured in the low-level troposphere of an intense hurricane near and inside an intense eyewall. Another observation of this kind was the flight-level data collected on 6 August 1980 in Hurricane Allen (1980). The data from these two flights provide a unique opportunity to estimate the characteristics of the turbulence near and underneath the eyewall of an intense storm. One objective of this study is to estimate turbulence parameters such as momentum flux, turbulent kinetic energy (TKE), and eddy diffusivity in the high-wind regime whose surface wind speeds exceed 30 m s^{-1}. Another objective is to estimate the spatial scales of the energy-containing turbulent eddies in the low-level eyewall using detailed spectral analysis.

An outline of the remaining sections of this paper is as follows. In section 2, we give a brief description of data and the analysis methodology. Section 3 describes the potential errors involved in the data analysis and the method employed herein to assure quality control. In section 4, we present the results of the spectral analysis. Section 5 presents the results of the estimated turbulence parameters and a detailed error analyses. This is followed by section 6, which summarizes the main findings and the limitations of the results.

2. Data and analysis method

As mentioned earlier, the data used in this study are from two research flights, one into category 4 Hurricane Allen (1980) and the other in category 5 Hurricane Hugo (1989). We analyzed the flight-level data from the period of missions before and during the eyewall penetrations when N42RF was flown at nearly constant radar altitudes below 1 km. Wind velocity data were corrected for aircraft motion, measured with an Inertial Navigation System (INS), and a Global Positioning System (GPS). Surface (10 m) wind speeds are estimated using measurements from a nadir-pointing stepped frequency microwave radiometer (SFMR; Uhlhorn et al. 2007). Note that there is no SFMR data during the flight mission into Hurricane Allen because SFMR was not installed at that time.

The data from the flight in Hurricane Hugo on 15 August 1989 have been published recently by Marks et al. (2008). That study provided a detailed description of the synoptic conditions, storm structure, the experiment, and data quality, etc. In this work, we used the data from the portion of the mission between 1720 and 1729 UTC. Flight-level parameters of interest include aircraft altitude and wind speed in the three Cardinal directions (Fig. 1). Also shown in Fig. 1 is the surface wind speed estimated by the SFMR. The gray lines in each panel of Fig. 1 represent the three time intervals investigated here. The first time interval was taken outside the eyewall and was chosen to compare against the results from CBLAST. The second time interval corresponds to the eyewall penetration up to the inner edge of the eyewall. Although this flight segment includes the rapid increase in the tangential wind with decreasing radius, it excludes the EVM. The third time interval covers both the eyewall penetration and the EVM. Time intervals 1 and 2 are judged suitable for turbulent flux calculations according to the detailed spectral analysis that will be discussed in sections 3 and 4. Time interval 3 on the other hand is not suitable for flux calculation, but it is nonetheless used for comparison purposes to estimate how the EVM may affect the three-dimensional turbulence characteristics.

The data used in this study from the flight in Hurricane Allen on 6 August have not been well documented in previous studies, except that the vertical velocity data had been used by Jorgensen et al. (1985). Hurricane Allen originated from a tropical wave that previously moved off the African coastline on 30 July. It formed as a tropical depression on 1 August, moving toward the west at nearly 20 mph. The storm became a category 5 storm south of Puerto Rico on 5 August and stayed at that strength for longer than a day. It weakened to a category 4 hurricane on 6 August but regained category 5 intensity again over a day. As Allen entered the Gulf it weakened back to a category 4 but once again quickly attained category 5 status. During six of the seven days (4–10 August 1980) when Hurricane Allen was in the

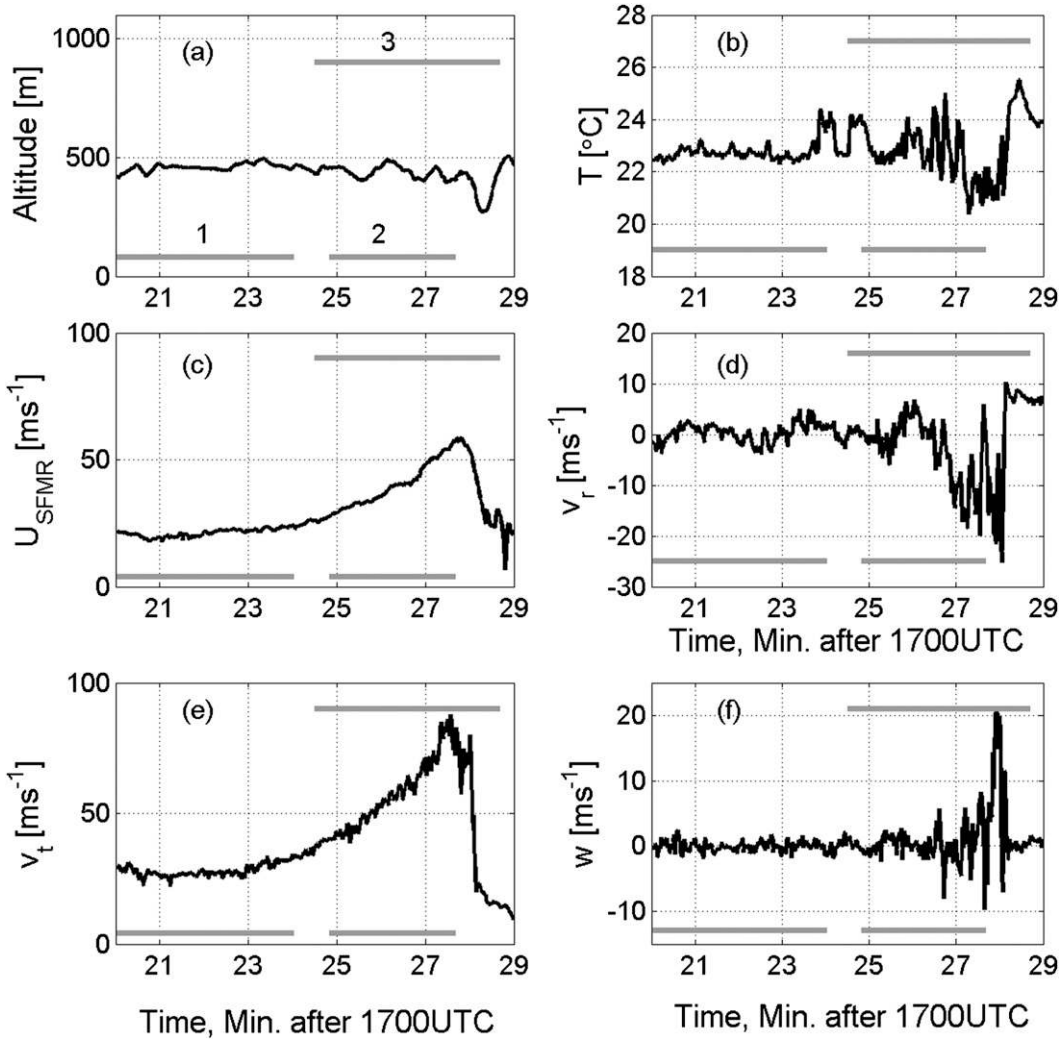

FIG. 1. Plots of (a) aircraft altitude, (b) temperature, (c) surface wind speed, (d) radial wind velocity, (e) tangential wind velocity, and (f) vertical velocity during Hurricane Hugo at 1720–1729 UTC 15 Sep 1989. The gray lines denote the three time intervals investigated.

Caribbean and Gulf of Mexico, a total of seven research missions were conducted by the two NOAA P3 aircraft (N42RF and N43RF). An overview of the synoptic conditions and a detailed account of the field programs can be referred to Jorgensen (1984) and Marks (1985).

Figure 2 shows the horizontal aircraft track that is superimposed on a composite radar reflectivity image that is from Marks (1985). Also shown in Fig. 2 is the aircraft altitude as a function of time in UTC. During the period between 1500 to 1640 UTC, N42RF was flown at a nearly constant altitude of around 450 m. Until 1650 UTC, the aircraft remained below 1 km above the sea surface. Figure 3 shows the variables of interest during the low-level mission. The gray lines at the bottom of each panel represent the time intervals selected to determine the scales of turbulent eddies and turbulence parameters. There are a total of 12 time intervals (or flux runs) selected for analysis, four of which are in the eyewall region. The remaining time intervals were taken outside the eyewall, and most of them correspond to times that the aircraft was between the outer rainbands. These remaining time intervals are used to compare with the CBLAST data at similar altitudes. Note that all the time intervals are chosen according to the ogive criterion discussed in section 3.

From the radial wind velocity, we can see that N42RF was flown mostly within the inflow layer for the periods of interest for both the Allen and Hugo flights. However, we are uncertain if the flights were within the hurricane boundary layer because there is no vertical sounding observation in both cases. According to previous studies examining vertical profiles of kinematic variables in

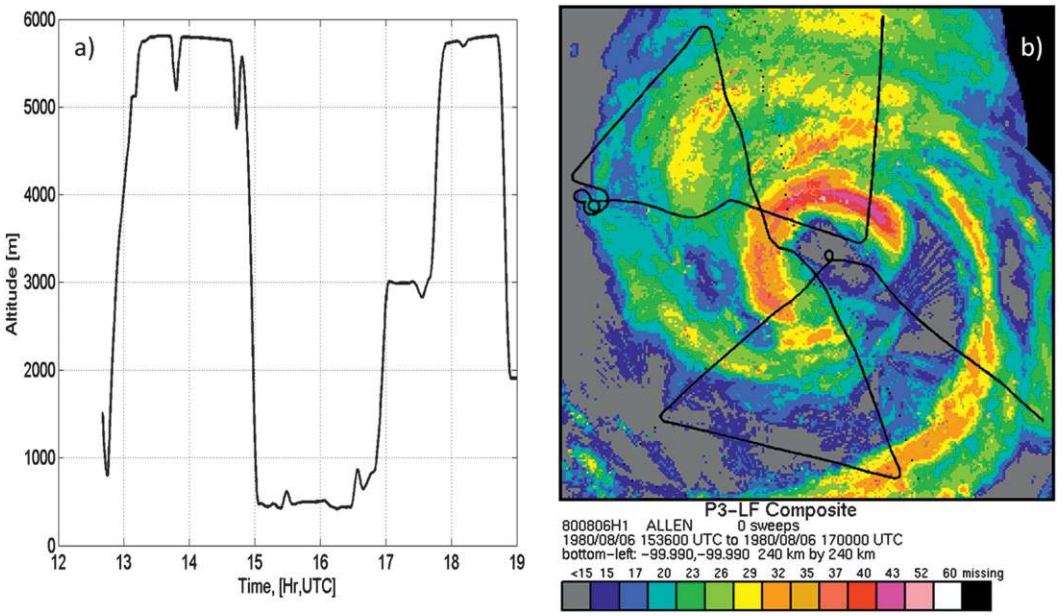

FIG. 2. Plots of (a) aircraft altitude and (b) horizontal aircraft track that is superimposed on top of a composite of a radar reflectivity image from Marks (1985), on 6 Aug 1980 in Hurricane Allen.

intense hurricane eyewalls (e.g., Franklin et al. 2003; Powell et al. 2003), it is likely that N42RF was near the height of the maximum wind speed. We assume that N42RF is close to the top of the boundary layer for the remainder of the paper (e.g., Kepert and Wang 2001; Bell and Montgomery 2008; Smith et al. 2009; Zhang et al. 2009; Smith and Montgomery 2010).

Tables 1 and 2 , respectively, summarize the measurements and calculations for the time intervals of the flights into Hurricanes Hugo and Allen. Overall, the time-averaged mean wind speeds obtained at flight level vary from 7 to 64 m s^{-1}. For the Hugo flight, the averaged near-surface wind speeds (U_{SFMR}), determined from measurements by the SFMR, vary from 21 to 40 m s^{-1}. The stability parameter, z/L, is also shown in Tables 1 and 2, where z is the aircraft altitude, and L is the Obukhov length calculated using an iterative method (Drennan et al. 2007); the results indicate that the thermodynamic conditions were near neutral but slightly unstable in the boundary layer. When estimating L, we use the surface exchange coefficients of momentum and heat from Powell et al. (2003) and Zhang et al. (2008) to estimate surface fluxes. It is assumed also that the sea surface temperature is 28°C. For the data in Hurricane Allen, there are no surface wind data, and we only have data at one level, so L was not estimated.

Turbulent fluxes of momentum at flight level are calculated using the eddy-correlation method for each time interval as follows:

$$\hat{\tau} = \rho(-\overline{w'v_t'}\,\hat{i} - \overline{w'v_r'}\,\hat{j}), \tag{1}$$

where prime indicates turbulent fluctuations; w, v_t, and v_r represent vertical, tangential, and radial component velocities, respectively; ρ is the air density; and an overbar represents a time-averaged operator. TKE is computed using the turbulent fluctuations in the form of

$$e = \frac{1}{2}(\overline{v_t'^2} + \overline{v_r'^2} + \overline{w'^2}). \tag{2}$$

Note that enthalpy fluxes cannot be estimated in this study because of the sensor limitation in measuring humidity and potential wetting of the temperature sensor.

Turbulent fluctuations are determined by detrending the time series of the three wind components using a least squares fitting method. A high-pass filter with a cutoff at 0.01 Hz was applied before the detrending. When we calculate ρ, we use the temperature measured by the Rosemont temperature sensor. It has been reported by Eastin et al. (2002a,b) that there is usually a wetting error in the temperature data during eyewall penetrations. We corrected the wetting error following the Eastin et al. method. We found that the influence of the wetting error on the density calculation is very small (~1%), which is nearly negligible.

Because the vertical eddy diffusivity is a key parameter in a number of planetary boundary layer (PBL) parameterization schemes used in numerical as well as

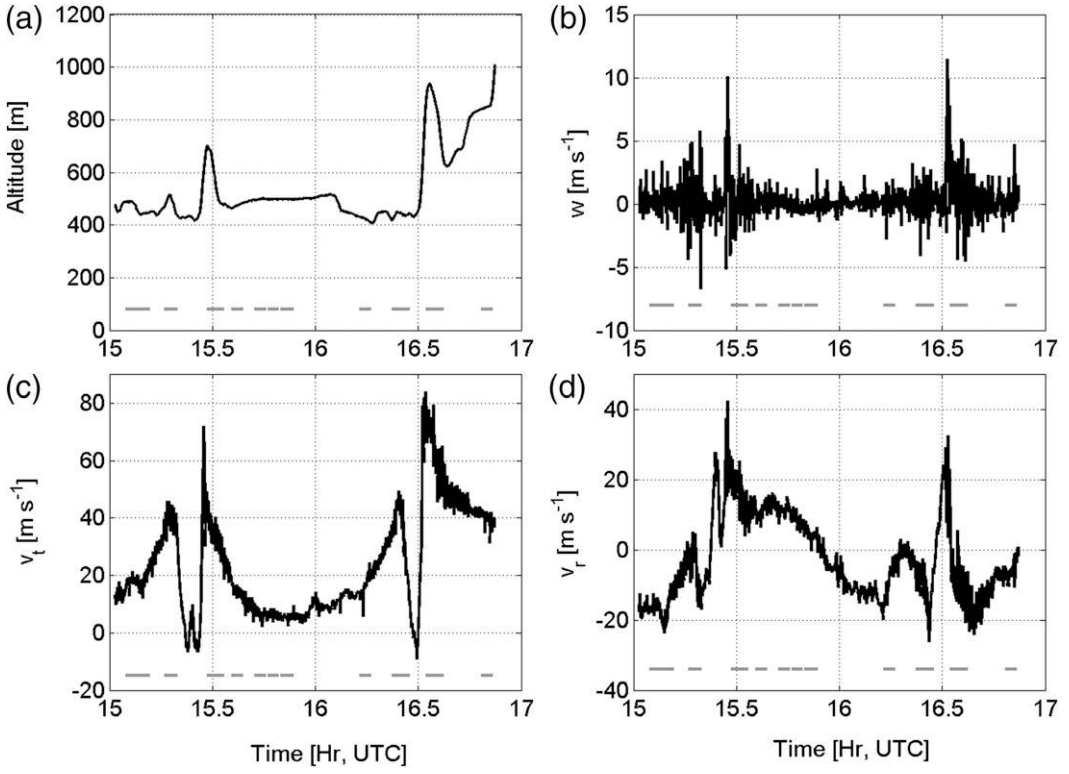

FIG. 3. Plots of (a) aircraft altitude, (b) vertical velocity, (c) tangential wind velocity, and (d) radial wind velocity during Hurricane Allen at 1501–1650 UTC 6 Aug 1980. The gray lines denote the time intervals investigated.

most theoretical models of hurricanes (e.g., Kepert 2001; Smith et al. 2008; Bryan and Rotunno 2009b; Smith and Thomsen 2010), we believe it worthwhile to estimate the vertical diffusivity here using the data in Hurricanes Hugo and Allen. Typically, the vertical eddy diffusivity is defined as

$$K = |\hat{\tau}|\left(\frac{\partial V}{\partial z}\right)^{-1}, \tag{3}$$

where V is the mean wind speed, and z is the altitude. We refer to Eq. (3) as the direct method hereafter. In this method for estimating K, one needs to calculate the vertical wind shear. For the case of Hurricane Hugo when the SFMR wind data are available, the wind shear is estimated from the difference between the flight-level winds and the surface winds. However, for the Allen case we could not estimate K using the direct method.

Previous studies (e.g., Hanna 1968) provided an alternative method for estimating K in the form of

$$K_1 = cl\sigma_w, \tag{4}$$

where σ_w is the standard deviation of the vertical wind velocity, l is the vertical mixing length scale defined as $l = \sigma_w^3/\varepsilon$, and c is a constant. Here, we use $c = 0.41$

TABLE 1. Summary of data and calculations for the three time intervals (1, 2, and 3) in Hurricane Hugo on 15 Sep 1989. The variables are as follows: the number of the time intervals (#); start time of the time interval (T_s in UTC hours and minutes); end time of the time interval (T_{nd}); mean altitude (z in m); mean flight-level wind speed (U_z in m s^{-1}); mean 10-m wind speed (U_{SFMR}); stability (where L is the Obukhov length); momentum flux ($|\tau|$ in N m^{-2}); dissipation rate (ε in cm^2 s^{-3}); TKE (e in m^2 s^{-2}); standard deviation of the vertical velocity (σ_w in m s^{-1}); vertical mixing length scale (l in m); peak horizontal length scale (l_{phl} in m); and vertical eddy diffusivity (K in m^2 s^{-1}). Here, K, K_1, and K_2 are the eddy diffusivity estimated using the direct method, Hanna's method, and the TKE closure method, respectively. Time interval 2 is in the eyewall. Note that time interval 3 is not a good run for flux calculation. The results for time interval 3 are given only for comparison purposes, which should not be used to evaluate model simulation outputs.

#	T_s	T_{nd}	z	U_z	U_{SFMR}	z/L	$\|\tau\|$	e	σ_w	ε	l	l_{phl}	K_1	K_2	K
1	1720	1724	463	28.2	21.5	−0.44	0.34	4.46	0.84	81.1	74.5	2490.7	25.6	26.3	23.1
2	1725	1728	436	59.0	40.0	−0.06	4.70	25.8	2.68	1778	108.6	2189.2	118.6	116.7	109.4
3	1724	1729	422	52.2	39.1	−0.08	26.2	258.2	4.80	5001	221.0	2142.8	435.7	497.6	824.0

TABLE 2. Summary of data and calculations for the 12 time intervals in Hurricane Allen on 6 Aug 1980. The variables are as follows: #; T_s (in UTC hours and minutes); T_{nd}; z (in m); U_z (in m s^{-1}); $|\tau|$ (in N m^{-2}); ε (in cm^2 s^{-3}); TKE (e in m^2 s^{-2}); σ_w (in m s^{-1}); l (in m); l_{phl} (in m); and K (in m^2 s^{-1}). K_1 and K_2 are the eddy diffusivity estimated using Hanna's method and the TKE closure method, respectively. Note that time intervals 9–12 are the ones in the eyewall.

#	T_s	T_{nd}	z	U_z	$\|\tau\|$	e	σ_w	ε	l	l_{phl}	K_1	K_2
1	1505	1508	482.6	24.5	0.28	1.65	0.78	76.0	63.6	900.3	24.9	10.8
2	1508	1512	442.6	25.1	0.53	3.36	0.96	132.8	66.0	911.4	47.8	25.5
3	1536	1539	473.0	18.6	0.13	1.75	0.70	34.4	98.1	888.2	11.5	26.7
4	1542	1545	497.8	13.3	0.11	1.32	0.48	26.9	40.7	1812.1	10.2	19.4
5	1546	1549	498.5	11.0	0.21	1.39	0.54	56.3	28.7	1904.7	18.6	10.3
6	1550	1553	498.3	7.2	0.12	1.57	0.63	132.3	19.0	3040.5	10.8	5.6
7	1613	1616	422.1	19.3	0.41	3.37	0.93	64.4	125.2	859.9	18.3	52.8
8	1648	1652	847.7	40.1	0.88	4.06	1.18	94.6	86.9	2947.6	20.5	26.1
9	1517	1520	484.6	39.7	2.74	13.1	2.20	1243	85.7	951.3	77.3	41.7
10	1528	1533	631.1	37.9	0.99	10.7	1.66	399	114.6	2521.2	78.0	86.7
11	1623	1627	448.7	40.9	1.76	15.7	2.46	1191	125.0	1760.1	126.1	62.1
12	1632	1637	844.9	64.2	2.89	20.0	2.38	1900	71.0	763.1	69.2	62.4

following Nieuwstadt (1984). Equation (4) will be hereafter referred to as Hanna's method.[1] Although Hanna's method is well suited for boundary layers where similarity theory is a plausible approximation, this method has been used successfully in other conditions, such as in the boundary layer over the forests where conditions are not homogeneous (Lee 1996). In this study, we will assume that Hanna's method can be used also in the low-level troposphere in hurricane conditions. The limitations of our estimates are discussed in sections 5 and 6.

The rate of dissipation ε is usually estimated from the velocity spectra in the form of

$$\varepsilon = \alpha^{-3/2}\frac{2\pi f}{U}[fS(f)]^{3/2}, \tag{5}$$

where f is the frequency, α is the one-dimensional Kolmogorov constant, U is the true airspeed relative to the aircraft, and S is the power spectral density of the along-wind component wind velocity. In this study, we conservatively use $\alpha = 0.5$ following the laboratory guidance provided by Sreenivasan (1995). In the estimation of ε, we assume the presence of an inertial subrange in the power spectrum.

In the PBL parameterization schemes used in numerical models, especially in the TKE closure–type schemes (Holt and Raman 1988), eddy diffusivity is usually related to TKE and the rate of dissipation, in the form of

$$K_2 = c_2 e^2/\varepsilon, \tag{6}$$

where c_2 is an empirical parameter. Here, we use $c_2 = 0.03$, following Detering and Etling (1985), Beljaars et al. (1987), and Lee (1996). Again, in Eq. (6) the estimation of K involves the estimation of the rate of dissipation, which we believe to have the largest uncertainty among all of the above-mentioned parameters. The uncertainty involved in the estimation of these turbulence parameters is discussed in sections 3 and 5.

3. Quality control and potential errors in the data analysis

The most important issue to note is that the flight-level data used in this study have a sampling rate of 1 Hz. Although these data were used widely in previous studies to understand various aspects of hurricane dynamics, thermodynamics, and vortex structure (e.g., Willoughby et al. 1982; Jorgensen 1984; Willoughby 1990; Kossin and Eastin 2001; Eastin et al. 2005a,b; Mallen et al. 2005), they have been rarely used to estimate turbulence properties. One potential major concern with the 1-Hz data for turbulence studies is the sampling problem—that is, the 1-Hz data cannot ordinarily capture the whole spectrum of the turbulent energy. This limitation notwithstanding, we believe that the 1-Hz data such as those collected in Hurricanes Hugo and Allen still have their merit for estimating turbulence parameters. Our belief is supported by a detailed comparison of the momentum fluxes, variances, and TKEs estimated using the 1- and 40-Hz data for identical flux runs during the CBLAST experiment.

As an example, Fig. 4 shows a comparison between the wind data with 1- and 40-Hz sampling frequencies. The data shown in Fig. 4 are from a flux run that was collected by NOAA N43RF aircraft in Hurricane Frances at 1920 UTC 1 September 2004. The measurements were taken between the outer rainbands of Hurricane Frances

[1] This is expected also from basic turbulence phenomenology (e.g., Frisch 1996).

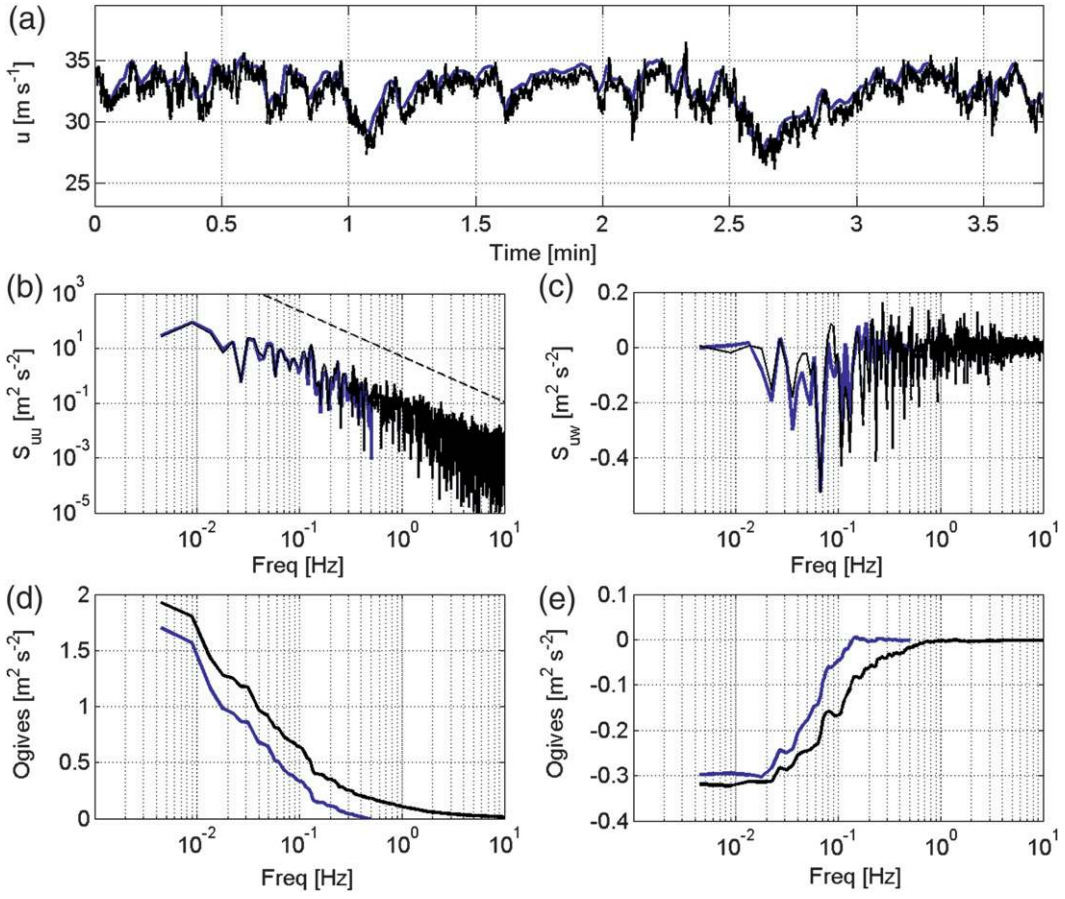

FIG. 4. Comparison of the 40- (black) and 1-Hz (blue) wind data. (a) Time series comparison from a typical flux run at 460 m on 1 Sep 2004 in Hurricane Frances. (b) Frequency spectra from the flux run of (a). (c) Frequency cospectra of *uw*. (d) Cumulative sum or ogive of the spectra. (e) Cumulative sum or ogive of cospectra.

as part of the CBLAST mission. The mean flight-level wind speed of this flux run is 32 m s^{-1}. The flux data for this flight has been presented elsewhere by Zhang et al. (2009). We note that this flight is the only one that has measurements between 400 and 500 m during CBLAST.

The time series of the along-wind component wind velocity u in 1 and 40 Hz are compared in Fig. 4a; the analyzed data show good agreement. The spectra and cospectra comparisons are shown next in Figs. 4b and 4c, respectively. We see that there is a good agreement in the spectra and cospectra between the 1- and 40-Hz data at frequencies <0.5 Hz, the equivalent of the Nyquist frequency for 1-Hz data. It is noticed that there is a tendency for the 1-Hz data to decay faster at a frequency range between 0.4 and 0.5 Hz. Beyond the Nyquist frequency, however, the 1-Hz data is unable to measure turbulent eddies smaller than around 200 m in space. Now, to estimate the spatial scales of the turbulent eddies, we first applied Taylor's frozen hypothesis to transfer the frequency to the wavenumber domain, defined as the frequency divided by the true airspeed relative to the aircraft, which is on the order of 100–150 m s^{-1}. The scale is then the reciprocal of the wavenumber.

The cumulative spectral and cospectral sums, or "ogives," are shown in Figs. 4d and 4e, respectively. The ogive plots have been widely used in turbulence studies to determine useful time intervals suitable for turbulent flux calculations (e.g., Zhang et al. 2009). The use of ogive curves when estimating fluxes provides insight into turbulent structure and spatial scales that contribute to the turbulent transport. The flatness of the ogive curve at low- and high-end frequencies indicates that the energy-containing scale of the variance and flux processes are well sampled. If the ogive curve approaches asymptotically a single value, then homogeneity or stationarity of the flow is met, and the asymptotic value of the ogive represents the total variance and covariance or flux of momentum. Upon examining Figs. 4d and 4e, we see that the total variance and covariance are

TABLE 3. Summary of data and calculations for the 10 time intervals in Hurricane Frances on 1 Sep 2004. The variables are as follows: #; T_s (in UTC hours and minutes); T_{nd}; z (in m); U_z (in m s^{-1}); $|\tau|$ (in N m^{-2}); ε (in cm^2 s^{-3}); TKE (e in m^2 s^{-2}); σ_w (in m s^{-1}); l (in m); and K (in m^2 s^{-1}). The subscript 1 represents 1-Hz data, and subscript 40 represents 40-Hz data. K_1 and K_2 are the eddy diffusivity estimated using Hanna's method and the TKE closure method, respectively. Vertical mixing length and Ks are calculated using the 40-Hz data.

#	T_s	T_{nd}	z	U_{z1}	U_{z40}	e_1	e_{40}	$\lvert\tau\rvert_1$	$\lvert\tau\rvert_{40}$	σ_{w1}	σ_{w40}	ε_1	ε_{40}	l	K_1	K_2
1	1743	1746	484.1	20.6	20.3	0.83	1.14	0.05	0.08	0.21	0.48	7.8	25.1	44.7	7.6	15.5
2	1747	1750	477.6	20.6	20.3	0.77	1.25	0.15	0.19	0.23	0.65	11.2	25.5	106.3	16.5	18.4
3	1751	1754	484.5	21.0	20.4	0.79	1.36	0.21	0.24	0.38	0.80	11.6	30.6	144.2	42.2	15.6
4	1755	1759	484.1	22.2	21.6	1.19	1.81	0.27	0.44	0.40	0.81	11.6	15.6	336.3	39.4	63.0
5	1801	1805	451.2	21.2	21.7	1.16	1.78	0.19	0.23	0.31	0.87	39.5	65.4	102.1	20.4	14.5
6	1907	1910	563.2	29.4	28.8	2.41	3.33	0.53	0.65	0.61	1.03	44.2	97.6	113.2	57.8	34.1
7	1911	1913	529.7	33.4	32.7	1.28	1.71	0.18	0.26	0.33	0.67	8.0	11.7	253.5	22.8	74.5
8	1914	1917	498.4	33.2	32.6	1.04	1.57	0.22	0.24	0.36	0.80	17.0	29.1	173.4	21.3	25.4
9	1917	1921	486.7	32.9	32.2	1.86	2.43	0.39	0.51	0.56	0.92	28.7	52.3	147.5	45.7	33.8
10	1925	1928	467.0	33.3	33.7	2.18	4.05	0.31	0.47	0.42	1.07	133.0	231.9	52.1	42.4	21.3

comparable to each other for the 1- and 40-Hz data. It is evident also that the 1-Hz data somewhat underestimates the variance and covariance.

On average, we found that the 1-Hz Frances data capture approximately 75% of the total momentum flux and 70% of the TKE (Table 3). In the analysis of the Allen and Hugo data, an empirical correction is applied to the flux and TKE calculations to compensate for the bias determined from the Frances data. We have assumed that the turbulence characteristics at the similar vertical levels and locations in Frances, Hugo, and Allen behave in a similar manner. We recognize that there is uncertainty in the correction, especially in the eyewall region where the 40-Hz data are unavailable, but this approach provides our best estimates.

Boundary layer turbulence studies usually assume that turbulent properties such as variances and fluxes are ensemble averages such that the average of a number of individual samples of data is under identical conditions. In aircraft measurements, it is generally assumed also that time or space averages converge to ensemble averages when the averaging time becomes sufficiently long or the averaging length becomes sufficiently large (e.g., Wyngaard 1986; Lenschow 1986). In the present case, the time intervals suitable for analysis are relatively short; these intervals were selected based on the quality control through the ogives criterion discussed above (further details are given in section 4). The short time interval used in the calculations can yield uncertainty of variance and covariance fluxes according to Mann and Lenschow (1994) and Mahrt (1998). We present the detailed error analysis in section 5 when we present the results of the estimated turbulence parameters.

4. Spectral analysis of eddy structure

The spectra of the three-dimensional wind velocities for the three time intervals in Hurricane Hugo are plotted in Fig. 5. Note that Marks et al. (2008) conducted spectral analysis for the whole leg that contains the three time intervals. Here, a more detailed spectral analysis for each of the three time intervals is shown separately. Figure 5 indicates that the spectra of the three-component wind velocity for all the three time intervals tends to follow the $-5/3$ Kolmogorov law at frequencies >0.2 Hz. Because the time intervals of the eyewall penetrations are in the crosswind direction, we cannot determine if there is a ratio of $4/3$ between the cross-stream and along-stream velocity spectra (Zhang 2010). To estimate the turbulent dissipation rate using Eq. (4), we must assume that the inertial subrange exists. It is evident in Fig. 5 that the peak energy in the wind velocity spectra increases somewhat from time intervals 1 to 3. This increase of energy in the spectra is consistent with the increase of the rate of dissipation from intervals 1 to 3, as shown in Table 1.

The cospectra of the v_t and v_r components of the momentum fluxes for time intervals 1 and 2 of Hurricane Hugo flight are shown next in Figs. 6a and 6b, respectively. The corresponding ogives of the cospectra are shown in Figs. 6c and 6d. To estimate the spatial scale of turbulent eddies, we plot the cospectra and ogives in the wavenumber domain. Since the ogive curves are nearly flat at low and high wavenumbers, this supports the assumption of the stationarity for time intervals 1 and 2. The dominant peaks in the cospectral plots are associated with turbulent eddies that contain most of the momentum fluxes. As mentioned earlier, the scales of the dominant eddies can be estimated as the reciprocal of the wavenumbers. During time interval 1 (Fig. 6a), for example, the peaks in the $v_t w$ cospectral plots at wavenumbers 4×10^{-4} m^{-1} and 6×10^{-4} m^{-1} correspond to length scales of approximately 2.5 and 1.4 km, respectively. During time interval 2 (Fig. 6b, the eyewall penetration leg), the dominant peaks of the $v_t w$ cospectra at wavenumbers 4.5×10^{-4} m^{-1} and 1.5×10^{-3} m^{-1}

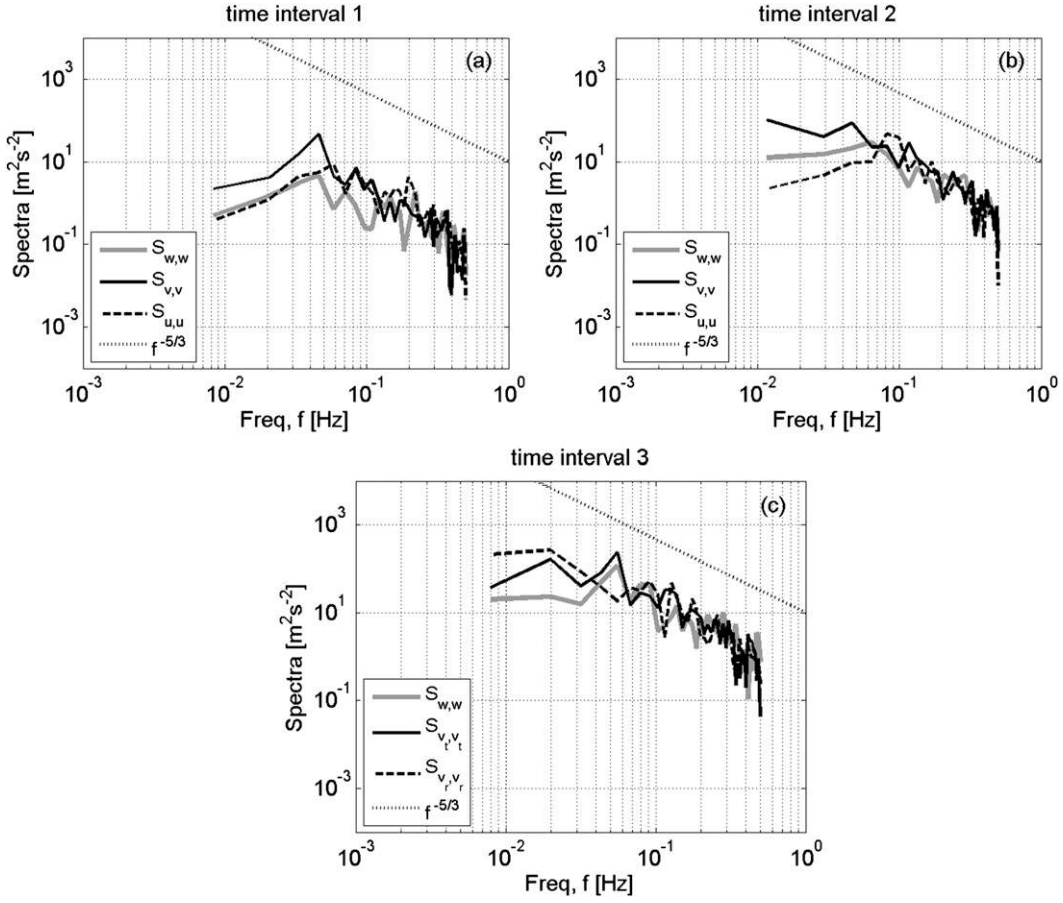

FIG. 5. Spectra of three velocity components for time intervals (a) 1, (b) 2, and (c) 3 in Hurricane Hugo. The dotted line shows a $-5/3$ slope.

correspond to length scales of approximately 2.2 km and 670 m, respectively.

The cospectra and ogives plots for the four eyewall penetrations legs in Hurricane Allen are shown in Fig. 7. It is evident from the plotted data that the eddy structures in those legs are comparable to that found in the eyewall penetration leg of Hurricane Hugo. The dominant peaks of the $v_t w$ and $v_r w$ cospectra take place at scales of approximately 500–3000 m. From the corresponding ogive curves it appears also that eddies with such scales contribute most to the total momentum fluxes. Tables 1 and 2 list the peak horizontal length scales of dominant eddy for all the time intervals. The results suggest that there is no apparent dependence of the peak horizontal length scale on wind speed.

Figure 8 shows the cospectra of the momentum fluxes and the corresponding ogives for time interval 3 of the Hugo flight. From the ogive curves in Fig. 8b, the contribution of turbulent eddies to the total flux in the wavenumber range 1.9×10^{-4} m^{-1} to 3×10^{-3} m^{-1} increases as the wavenumber decreases. However, there is a sharp increase in the contribution to the total energy for wavenumber $<1.9 \times 10^{-4}$ m^{-1}, indicating that the vertical momentum transport is strongly influenced by the large-scale features, possibly the convective-scale eddies with scales >5 km. The inclusion of the EVM increases the total momentum flux by almost an order of magnitude compared to that of time interval 2. On the other hand, because of the sharp increase in the ogive plots, Fig. 8 indicates that time interval 3 is not a good run for the flux calculation. Based upon the discussion and interpretation presented in Marks et al. (2008), the EVMs appear to behave in some respects like quasi-two-dimensional vortex structures that are embedded within the three-dimensional turbulence on the inside edge of the eyewall. Such features are believed to have a transient nature but possess very intense signatures locally (Schubert et al. 1999; Kossin and Schubert 2001; Montgomery et al. 2002; Yau et al. 2004; Montgomery et al. 2006). If the EVMs were included in the turbulence analysis, the homogeneity or stationarity condition would not be satisfied, indicating that it is unwise to include EVM in the

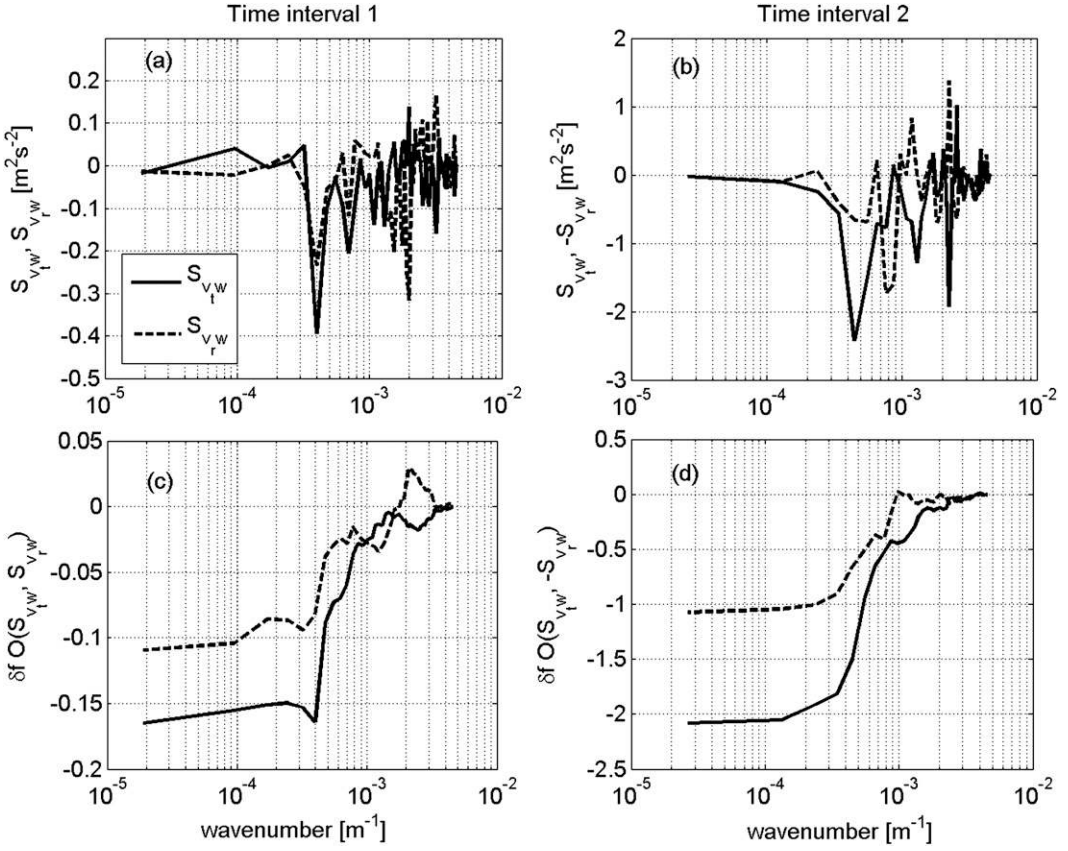

FIG. 6. Cospectra of the vertical velocity w with the tangential v_t and radial v_r velocity and the corresponding cumulative sums or ogives for time intervals 1 and 2, respectively, in Hurricane Hugo.

flux calculation. We point out here that we have listed the value of the vertical momentum flux for time interval 3 in Table 1 for comparison purposes only. We think that time interval 2 is more like a typical eyewall boundary layer leg at 450 m than time interval 3. Thus, the numerical-modeling community should be cautious when using the results of time interval 3 of the Hugo flight to compare with model output.

5. Estimation of turbulence parameters and error analysis

The calculations of TKE and momentum flux using Eqs. (1) and (2) are summarized in Tables 1 and 2, respectively, for the Hugo and Allen data. The data outside the eyewalls of Hurricanes Hugo and Allen show good agreement with the 40-Hz Frances data. This agreement suggests that the method employed for correcting the 1-Hz data is sound. The momentum flux for the eyewall penetration leg in Hurricane Hugo is approximately 4.7 N m^{-2} with a flight-level mean wind speed of 59 m s^{-1}. The mean momentum flux of the two eyewall legs at around 450 m for Hurricane Allen, with a flight-level mean wind speed of approximately 40 m s^{-1}, is 2.3 N m^{-2}. Overall, the momentum fluxes in the eyewall legs are generally 5–10 times those found in the outer-core runs. The TKE values for the eyewall legs fall between 10 and 25 m^2 s^{-2}; these values are consistent with the independently derived results of Lorsolo et al. (2010) who used Doppler radar data to map TKE in several hurricanes. The TKE in the eyewall region obtained using the flight-level data is roughly 7 times that in the legs outside the eyewall; this is also consistent with the Lorsolo et al. study.

Figures 9a and 9b show the TKE and momentum fluxes as a function of the flight-level mean wind speed, respectively. Also shown are the values of TKE and momentum fluxes determined from the 40-Hz data obtained in Hurricane Frances (2004). Based upon these results, it appears that the momentum flux and TKE increase with the increasing flight-level wind speed, confirming that the turbulent flux and energy are strongest in the eyewall region.

As mentioned in section 3, there are sources of error that are involved in the flux estimation. Following the

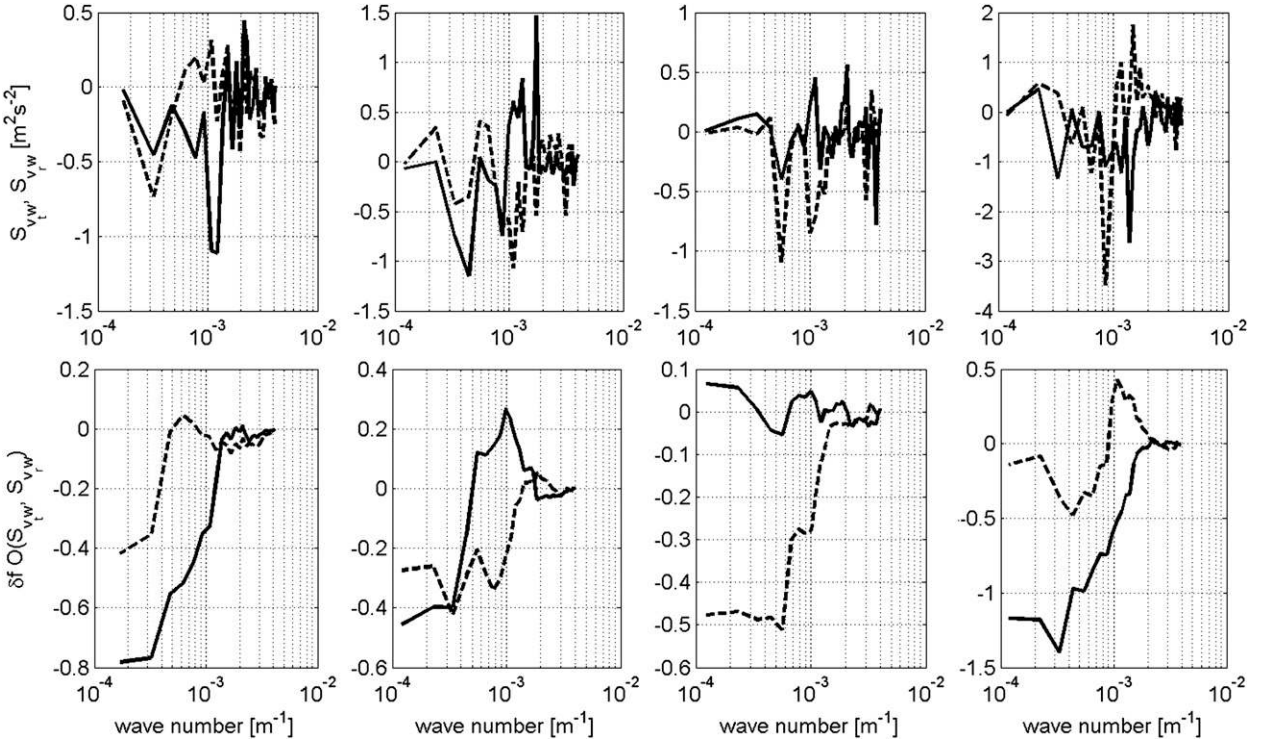

FIG. 7. As in Fig. 6, but for the (left to right) four time intervals 9, 10, 11, and 12 during the eyewall penetrations of Hurricane Allen.

method described by Drennan et al. (2007), the sampling error is given by

$$\sigma_F/\overline{F} = a_F z^{1/2} U_a^{-1/2} T^{-1/2}, \tag{7}$$

where σ_F is the standard deviation of flux estimates, a_F is a constant, U_a is the true airspeed relative to the airplane, T is the sampling interval (s), and z is the altitude (m). For momentum flux, Sreenivansan et al. (1978) estimated $a_F = 3$. The measurements in this study were carried out at altitudes between 430 and 800 m, with a true airspeed of $U_a \approx 120$ m s^{-1} and a short duration of $T \approx 180$ s. Using Eq. (7), the expected variability of the flux estimates using the Hugo and Allen data is then 85%. This variability is higher than the measured variability of 53% for the five eyewall legs and 74% for the legs outside the eyewall, suggesting that the analysis method used here is reasonable.

Two types of errors arise when estimating fluxes by the eddy-correlation method: the systematic error (erS), which is linked to the loss due to high-pass filtering; and random error (erR), which is due to the fact that a flight leg is a finite sample of a random process. We calculate the systematic error for the flux estimation following the methodology described by Mann and Lenschow (1994),

$$\text{erS} = (F - F_f)/F, \tag{8}$$

where F_f is the flux after the high-pass filter. The systematic error is found to be 28%, which is normal for aircraft observations especially at these altitudes. We estimate the random error following Vickers and Mahrt (1997),

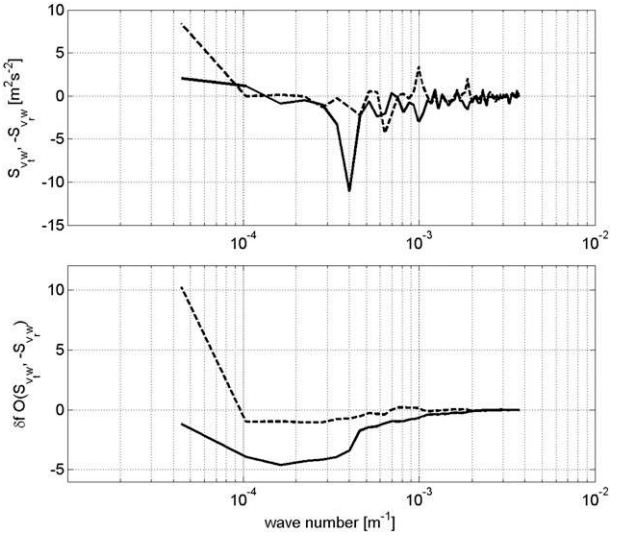

FIG. 8. As in Fig 6, but for time interval 3 in Hurricane Hugo.

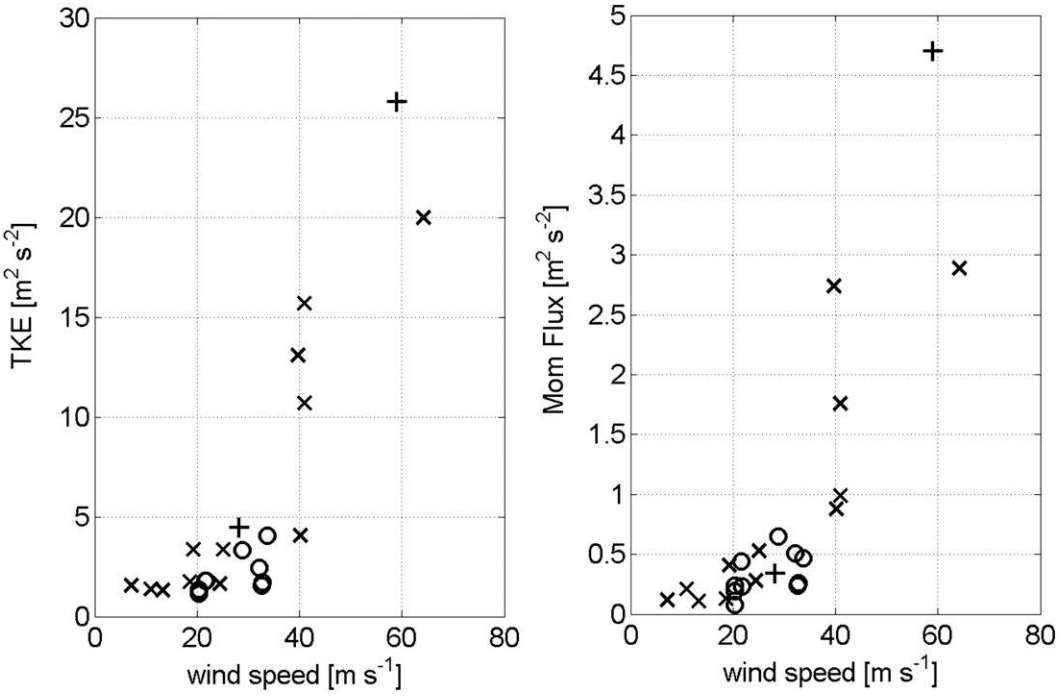

FIG. 9. Plots of TKE and momentum flux as a function of the mean wind speed at the flight level in Hurricanes Allen (×), Hugo (+), and Frances (○).

$$\mathrm{erR} = \sigma_F/\overline{F}/\sqrt{N}, \tag{9}$$

where N is the number of observations. The random error is found to be 24% for both the eyewall legs and those outside the eyewall, which is in agreement with values found in the literature (e.g., Mann and Lenschow 1994; Bernard-Trottolo et al. 2003). Because all the time intervals or flux runs were thoroughly checked using ogive criterion and the cumulative sum analysis method as mentioned in section 3, all of the low-frequency scales are captured. We have also corrected the missing high-frequency part of the energy based on the CBLAST data. At the end, the overall uncertainty of the estimated TKE and momentum flux is thought to be around 30%.

Using Hanna's method, we find that the vertical mixing length scale near the eyewall region is approximately 70–125 m. The mixing length estimated using the Frances data varies from 50–330 m. Similar values of mixing length are observed in the Allen and Hugo data in the outer-core region. In light of the large scatter of the data, we cannot deduce a wind speed dependence of the mixing length.

The vertical eddy diffusivity is estimated using the methods mentioned in section 2. Using the Hugo data, the eddy diffusivity estimated based on the three different methods are in reasonable agreement (Table 1). Using the Allen data, the Ks estimated using Hanna's method and the TKE closure method also agree with each other (Table 2).

In estimating K using the direct method [Eq. (3)], we estimated the vertical shear using the wind data at two levels. It is likely that we have overestimated the shear, given that the observation altitude may be close to the wind maximum where the shear is relatively low according to the eyewall dropsonde data shown by Franklin et al. (2003) and Powell et al. (2003). However, the data we used are outside the radius of the maximum wind speed, where the shear at 450 m is usually higher than that in the inner eyewall from previous case studies (e.g., Kepert 2006a,b; Schwendike and Kepert 2008). We believe that our estimation of the shear in Hurricane Hugo is realistic.

Figure 10 shows the Ks as a function of the mean flight-level wind speed, using the Hugo and Allen data as well as the 40-Hz Frances data. The Ks estimated only using the Frances data based on Hanna's method and the TKE closure methods show good agreement. We found that the Allen data and Hugo data in the outer-core region are close to the Frances data, giving some assurance of the validity of the bias correction. Considering all the data investigated in this work, it is evident that Ks in the eyewall regions are much larger than that those at the outer-core regions. For the eyewall legs,

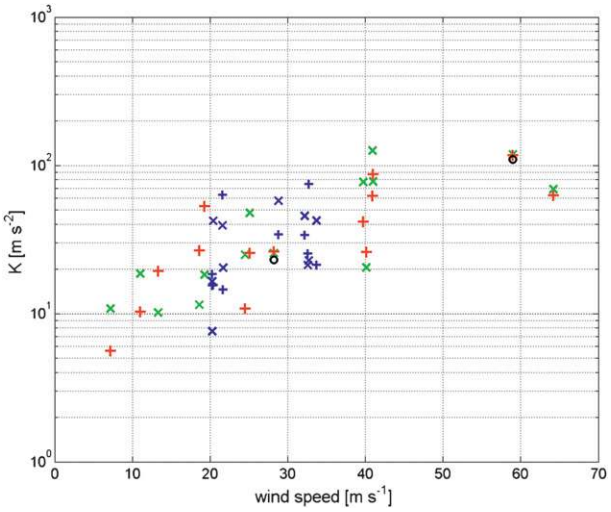

FIG. 10. Plots of the eddy diffusivity as a function of mean wind speed at the flight level for all the good runs in Hurricanes Allen, Hugo, and Frances. Here, *K*s are estimated using three methods: the direct method (○), Hanna's method (×), and the TKE closure method (+). The Frances data are in blue. The Hugo and Allen data are in the other color for different methods.

the *K*s vary between 70 and 130 $m^2 s^{-1}$ using Hanna's method, and they vary between 40 and 90 $m^2 s^{-1}$ using the TKE closure method. Overall, it is found that the eddy diffusivity tends to increase logarithmically with the increasing mean flight-level wind speed.

When using either Hanna's method or the TKE closure method, a large error arises in the estimation of the rate of dissipation. To reduce the uncertainty in the ε estimation, we applied a correction to the Hugo and Allen 1-Hz data based on the Frances 40-Hz data. After the correction, the Hugo and Allen data at the outer-core region agree with the Frances data. Given that there are no high-resolution (>10 Hz) data available, it is not possible to precisely ascertain the uncertainty in ε in the eyewall region. The authors are unaware of any other method for estimating *K* that does not rely on an estimation of ε, given the limited data used here. The uncertainty in the estimation of *K* using Hanna's method and the TKE closure method also comes from the empirical constants. For instance, we used $c = 0.41$ following Nieuwstadt (1984) for stable boundary layer, while the boundary layer we studied are nearly neutral. The overall uncertainty of the estimated *K* using Hanna's method and the TKE closure methods is thought to be around 50%.

6. Discussion and conclusions

In this study, the turbulence characteristics in the low-level troposphere (~450 m altitude) of Hurricanes Hugo (1989) and Allen (1980) have been investigated. Turbulent fluxes of momentum and TKE were estimated before and during the eyewall penetration. Momentum fluxes and TKE estimated for the eyewall penetration leg are found to be nearly an order of magnitude larger than those estimated for the legs outside the eyewall at the same level. The TKE and momentum fluxes are found to increase with increasing mean wind speed at the same level. The vertical mixing length scale is found to be approximately 100 m in the eyewall region, with slightly smaller values outside the eyewall.

Through spectral analysis, the spatial scales of dominant turbulent eddies in the eyewall penetration legs are found to lie between 500 and 3000 m. The turbulence in the hurricane boundary layer is three-dimensional from the spectral analysis. Our analyses indicate that it is unwise to include EVM in the turbulence parameter estimation.

We also estimated the vertical eddy diffusivity *K* using three different methods: the first uses the definition of *K*, the second uses a theoretical method given by Hanna (1968), and the third uses a TKE closure method. Using these three methods, the estimated *K*s are generally consistent with one another using the Hugo data. The estimated *K*s using the later two methods for the Allen data also agree with each other. Based upon the reasonable agreement on the estimated *K*s using the Hugo and Allen data outside the eyewall with the CBLAST data in Hurricane Frances, we think our methodology for estimating *K* using the available data is sound. In the intense eyewall region, we found that *K* varies approximately from 40 to 130 $m^2 s^{-1}$.

Foster (2009) has pointed out that the solutions for a similarity model of the hurricane boundary layer are sensitive to the specification of *K*. This solution sensitivity arises not only from the magnitude of *K* but also the variation of *K* with altitude and radius. Our analyses suggest that *K* increases with increasing mean wind speed at the same level. The use of a constant *K* is not expected to reproduce realistic turbulent momentum fluxes in a hurricane boundary layer.

According to different turbulence parameterization methods used in previous theoretical and numerical studies of the hurricane boundary layer, the maximum *K* varies from 38 to 101 $m^2 s^{-1}$ (e.g., Smith 1968; Kepert 2001; Smith 2003; Foster 2009). This range is comparable to our estimate of *K* for the eyewall legs. On the other hand, the maximum *K* used in the Medium-Range Forecast Model (MRF) boundary layer scheme in MM5 exceeds 250 $m^2 s^{-1}$ in the eyewall region and still has values larger than 50 $m^2 s^{-1}$ at radii beyond 200 km (Braun and Tao 2000; Smith and Thomsen 2010). Based upon our analysis, the MRF scheme may be a bit too

diffusive, while the rest of the schemes may use a relatively plausible range of K. However, more observations in the high-wind regime are required in the future to evaluate the Ks used in idealized theoretical and operational hurricane numerical models.

It is certainly true that our method to estimate K is borrowed from the standard turbulence community for boundary layers in low-wind conditions where the turbulence characteristics are presumed homogeneous in the horizontal direction. A hurricane boundary layer near the eyewall region is clearly far from a homogeneous regime! In particular, when the transient and intense EVMs exist, the flow is strongly inhomogeneous. These points notwithstanding, we think standard turbulence phenomenology should still provide a reasonable estimate of the turbulent quantities using the real observational data. While an eddy-resolving numerical simulation of an intense hurricane offers an alternative approach for estimating the turbulent properties that is free of these limitations (Rotunno et al. 2009), this approach has its own challenges. We think our analyses provide a useful starting point for the evaluation of hurricane prediction models. Specifically, our results offer the opportunity to assess boundary layer parameterization schemes used in numerical models for predicting hurricane intensity.

One clear limitation of this work is the small sample of the data used in the analysis. In searching for the low-altitude flight-level database collected by the Hurricane Research Division during the last several decades, the Allen and Hugo flight-level datasets are believed to be among the few available in situ observations that were taken below 500 m during the eyewall penetration of a category 4 and 5 storms. *It is unfortunate for hurricane science that we may not see such data like those collected in Hurricanes Hugo and Allen in the near future because NOAA has forbidden these types of flights with manned aircraft for obvious safety reasons*. To fully assess the impact of turbulent processes on the prediction of hurricane intensification and maximum intensity, and to further understand the role of turbulence in the eyewall dynamics and thermodynamics of a hurricane, a dedicated field program is recommended, possibly with unmanned platforms employing advanced turbulent sensors on board.

Acknowledgments. This work was supported through NOAA HFIP program. JZ also acknowledges the support from the National Research Council Research Associateship Award. MTM acknowledges support by NOAA, ONR, and the Naval Postgraduate School in Monterey, California. We appreciate comments from Roger Smith, Mark Powell, and Joe Cione that have helped improve both thought and presentation. We also thank Mark Donelan and William Drennan for constructive suggestions. Finally, we thank two anonymous reviewers for their substantive comments.

REFERENCES

Beljaars, A. C. M., J. L. Walmsley, and P. A. Talor, 1987: A mixed spectral finite-difference model for neutrally stratified boundary layer flow over roughness changes and topography. *Bound.-Layer Meteor.,* **38,** 273–303.

Bell, M. M., and M. T. Montgomery, 2008: Observed structure, evolution, and intensity of category five Hurricane Isabel (2003) from 12–14 September. *Mon. Wea. Rev.,* **136,** 2023–2036.

Bernard-Trottolo, S., B. Campistron, A. Druilhet, F. Lohou, and F. Said, 2003: TRAC98: Detection of coherent structures in a convective boundary layer using airborne measurements. *Bound.-Layer Meteor.,* **111,** 181–224.

Black, P. G., and Coauthors, 2007: Air–sea exchange in hurricanes: Synthesis of observations from the coupled boundary layer air–sea transfer experiment. *Bull. Amer. Meteor. Soc.,* **88,** 357–374.

Braun, S. A., and W.-K. Tao, 2000: Sensitivity of high-resolution simulations of Hurricane Bob (1991) to planetary boundary layer parameterizations. *Mon. Wea. Rev.,* **128,** 3941–3961.

Bryan, G. H., and R. Rotunno, 2009a: Evaluation of an analytical model for the maximum intensity of tropical cyclones. *J. Atmos. Sci.,* **66,** 3042–3060.

——, and ——, 2009b: The maximum intensity of tropical cyclones in axisymmetry numerical model simulations. *Mon. Wea. Rev.,* **137,** 1770–1789.

Detering, H. W., and D. Etling, 1985: Application of the E-ϵ turbulence model to the atmospheric boundary layer. *Bound.-Layer Meteor.,* **33,** 113–133.

Drennan, W. M., J. A. Zhang, J. R. French, C. McCormick, and P. G. Black, 2007: Turbulent fluxes in the hurricane boundary layer. Part II. Latent heat fluxes. *J. Atmos. Sci.,* **64,** 1103–1115.

Eastin, M. D., P. G. Black, and W. M. Gray, 2002a: Flight-level thermodynamic instrument wetting errors in hurricanes. Part I: Observations. *Mon. Wea. Rev.,* **130,** 825–841.

——, ——, and ——, 2002b: Flight-level thermodynamic instrument wetting errors in hurricanes. Part II: Implications. *Mon. Wea. Rev.,* **130,** 842–851.

——, W. M. Gray, and P. G. Black, 2005a: Buoyancy of convective vertical motions in the inner core of intense hurricanes. Part I: General statistics. *Mon. Wea. Rev.,* **133,** 188–208.

——, ——, and ——, 2005b: Buoyancy of convective vertical motions in the inner core of intense hurricanes. Part II: Case studies. *Mon. Wea. Rev.,* **133,** 209–227.

Emanuel, K. A., 1995: Sensitivity of tropical cyclones to surface exchange coefficients and a revised steady-state model incorporating eye dynamics. *J. Atmos. Sci.,* **52,** 3969–3976.

——, 1997: Some aspects of hurricane inner-core dynamics and energetics. *J. Atmos. Sci.,* **54,** 1014–1026.

Foster, R. C., 2009: Boundary-layer similarity under an axisymmetric, gradient wind vortex. *Bound.-Layer Meteor.,* **131,** 321–344.

Franklin, J. L., M. L. Black, and K. Valde, 2003: GPS dropwindsonde wind profiles in hurricanes and their operational implications. *Wea. Forecasting,* **18,** 32–44.

French, J. R., W. M. Drennan, J. A. Zhang, and P. G. Black, 2007: Turbulent fluxes in the hurricane boundary layer. Part I: Momentum flux. *J. Atmos. Sci.,* **64,** 1089–1102.

Frisch, U., 1996: *Turbulence: The Legacy of A. N. Kolmogorov*. Cambridge University Press, 296 pp.

Hanna, S. R., 1968: A method of estimating vertical eddy transport in the planetary boundary layer using characteristics of the vertical velocity spectrum. *J. Atmos. Sci.,* **25,** 1026–1033.

Holt, T., and S. Raman, 1988: A review and comparative evaluation of multilevel boundary layer parameterization for first-order and turbulent kinetic energy closure schemes. *Rev. Geophys.,* **26,** 761–780.

Jorgensen, D. P., 1984: Mesoscale and convective scale characteristics of mature hurricanes. Part I: General observations by research aircraft. *J. Atmos. Sci.,* **41,** 1268–1285.

——, E. J. Zipser, and M. A. LeMone, 1985: Vertical motions in intense hurricanes. *J. Atmos. Sci.,* **42,** 839–856.

Kepert, J. D., 2001: The dynamics of boundary layer jets within the tropical cyclone core. Part I: Linear theory. *J. Atmos. Sci.,* **58,** 2469–2484.

——, 2006a: Observed boundary layer wind structure and balance in the Hurricane core. Part I: Hurricane Georges. *J. Atmos. Sci.,* **63,** 2169–2193.

——, 2006b: Observed boundary layer wind structure and balance in the Hurricane core. Part II: Hurricane Mitch. *J. Atmos. Sci.,* **63,** 2194–2211.

——, and Y. Wang, 2001: The dynamics of boundary layer jets within the tropical cyclone core. Part II: Nonlinear Enhancement. *J. Atmos. Sci.,* **58,** 2485–2501.

Kossin, J. P., and M. D. Eastin, 2001: Two distinct regimes in the kinematic and thermodynamic structure of the hurricane eye and eyewall. *J. Atmos. Sci.,* **58,** 1079–1090.

——, and W. H. Schubert, 2001: Mesovortices, polygonal flow patterns, and rapid pressure falls in hurricane-like vortices. *J. Atmos. Sci.,* **58,** 2196–2209.

Lee, X., 1996: Turbulence spectra and eddy diffusivity over forests. *J. Appl. Meteor.,* **35,** 1307–1318.

Lenschow, D. H., Ed., 1986: Aircraft measurements in the boundary layer. *Probing the Atmospheric Boundary Layer,* Amer. Meteor. Soc., 39–55.

Lorsolo, S., J. A. Zhang, F. D. Marks, and J. Gamache, 2010: Estimation and mapping of hurricane turbulent energy using airborne Doppler measurements. *Mon. Wea. Rev.,* **138,** 3656–3670.

Mahrt, L., 1998: Flux sampling errors from aircraft and towers. *J. Atmos. Oceanic Technol.,* **15,** 416–429.

Mallen, K. J., M. T. Montgomery, and B. Wang, 2005: Reexamining the near-core radial structure of the tropical cyclone primary circulation: Implications for vortex resiliency. *J. Atmos. Sci.,* **62,** 408–425.

Mann, J., and D. H. Lenschow, 1994: Errors in airborne flux measurements. *J. Geophys. Res.,* **99,** 14 519–14 526.

Marks, F. D., 1985: Evolution of the structure of precipitation in Hurricane Allen (1980). *Mon. Wea. Rev.,* **113,** 909–930.

——, P. G. Black, M. T. Montgomery, and R. W. Burpee, 2008: Structure of the eye and eyewall of Hurricane Hugo (1989). *Mon. Wea. Rev.,* **136,** 1237–1259.

Montgomery, M. T., V. A. Vladimirov, and P. V. Denissenko, 2002: An experimental study on hurricane mesovortices. *J. Fluid Mech.,* **471,** 1–32.

——, M. M. Bell, S. Aberson, and M. Black, 2006: Hurricane Isabel (2003): New insights into the physics of intense storms. Part I: Mean vortex structure and maximum intensity estimate. *Bull. Amer. Meteor. Soc.,* **87,** 1335–1347.

Moss, M. S., 1978: Low-level turbulence structure in the vicinity of a hurricane. *Mon. Wea. Rev.,* **106,** 841–849.

——, and F. J. Merceret, 1976: A note on several low-layer features of Hurricane Eloise (1975). *Mon. Wea. Rev.,* **104,** 967–971.

——, and ——, 1977: A comparison of velocity spectra from hot film anemometer and gust-probe measurements. *J. Appl. Meteor.,* **16,** 319–320.

Nieuwstadt, F. T. M., 1984: The turbulent structure of the stable nocturnal boundary layer. *J. Atmos. Sci.,* **41,** 2202–2216.

Nolan, D. S., J. A. Zhang, and D. P. Stern, 2009a: Evaluation of planetary boundary layer parameterizations in tropical cyclones by comparison of in-situ data and high-resolution simulations of Hurricane Isabel (2003). Part I: Initialization, maximum winds, and outer-core boundary layer structure. *Mon. Wea. Rev.,* **137,** 3651–3674.

——, ——, and ——, 2009b: Evaluation of planetary boundary layer parameterizations in tropical cyclones by comparison of in-situ data and high-resolution simulations of Hurricane Isabel (2003). Part II: Inner core boundary layer and eyewall structure. *Mon. Wea. Rev.,* **137,** 3675–3698.

Persing, J., and M. T. Montgomery, 2003: Hurricane superintensity. *J. Atmos. Sci.,* **60,** 2349–2371.

Powell, M. D., P. J. Vickery, and T. A. Reinhold, 2003: Reduced drag coefficient for high wind speeds in tropical cyclones. *Nature,* **422,** 279–283.

Rotunno, R., Y. Chen, W. Wang, C. Davis, J. Dudhia, and G. J. Holland, 2009: Large-eddy simulation of an idealized tropical cyclone. *Bull. Amer. Meteor. Soc.,* **90,** 1783–1788.

Schubert, W. H., M. T. Montgomery, R. K. Taft, T. A. Guinn, S. R. Fulton, J. P. Kossin, and J. P. Edwards, 1999: Polygonal eyewalls, asymmetric eye contraction, and potential vorticity mixing in hurricanes. *J. Atmos. Sci.,* **56,** 1197–1223.

Schwendike, J., and J. D. Kepert, 2008: The boundary layer winds in Hurricanes Danielle (1998) and Isabel (2003). *Mon. Wea. Rev.,* **136,** 3168–3192.

Smith, R. K., 1968: The surface layer of a hurricane. *Tellus,* **20,** 473–484.

——, 2003: A simple model of the hurricane boundary layer. *Quart. J. Roy. Meteor. Soc.,* **129,** 1007–1027.

——, and M. T. Montgomery, 2010: Hurricane boundary-layer theory. *Quart. J. Roy. Meteor. Soc.,* **136,** 1665–1670.

——, and G. L. Thomsen, 2010: Dependence of tropical-cyclone intensification on the boundary layer representation in a numerical model. *Quart. J. Roy. Meteor. Soc.,* **136,** 1671–1685.

——, M. T. Montgomery, and S. Vogl, 2008: A critique of Emanuel's hurricane model and potential intensity theory. *Quart. J. Roy. Meteor. Soc.,* **134,** 551–561.

——, ——, and S. V. Nguyen, 2009: Tropical cyclone spin-up revisited. *Quart. J. Roy. Meteor. Soc.,* **135,** 1321–1335.

Sreenivasan, K. R., 1995: On the universality of the Kolmogorov constant. *Phys. Fluids,* **7,** 2778–2784.

——, A. J. Chambers, and R. A. Antonia, 1978: Accuracy of moments of velocity and scalar fluctuations in the atmospheric surface layer. *Bound.-Layer Meteor.,* **14,** 341–359.

Uhlhorn, E. W., P. G. Black, J. L. Franklin, M. Goodberlet, J. Carswell, and A. S. Goldstein, 2007: Hurricane surface wind measurements from an operational stepped frequency microwave radiometer. *Mon. Wea. Rev.,* **135,** 3070–3085.

Vickers, D., and L. Mahrt, 1997: Quality control and flux sampling problems for tower and aircraft data. *J. Atmos. Oceanic Technol.,* **14,** 512–526.

Willoughby, H. E., 1990: Gradient balance in tropical cyclones. *J. Atmos. Sci.,* **47,** 265–274.

——, J. A. Clos, and M. G. Shoreibah, 1982: Concentric eyewalls, secondary wind maxima, and the evolution of the hurricane vortex. *J. Atmos. Sci.,* **39,** 395–411.

Wyngaard, J. C., 1986: Measurements physics. *Probing the Atmospheric Boundary Layer,* D. H. Lenschow, Ed., Amer. Meteor. Soc., 5–18.

Yau, M. K., Y. Liu, D.-L. Zhang, and Y. Chen, 2004: A multiscale numerical study of Hurricane Andrew (1992). Part VI: Small-scale inner-core structures and wind streaks. *Mon. Wea. Rev.,* **132,** 1410–1433.

Zhang, J. A., 2010: Spectral characteristics of turbulence in the hurricane boundary layer over the ocean between the outer rainbands. *Quart. J. Roy. Meteor. Soc.,* **136,** 918–926.

——, P. G. Black, J. R. French, and W. M. Drennan, 2008: First direct measurements of enthalpy flux in the hurricane boundary layer: the CBLAST results. *Geophys. Res. Lett.,* **35,** L14813, doi:10.1029/2008GL034374.

——, W. M. Drennan, P. G. Black, and J. R. French, 2009: Turbulence structure of the hurricane boundary layer between the outer rainbands. *J. Atmos. Sci.,* **66,** 2455–2467.